Structural Engineering and Mechanics, *Vol. 60, No. 3 (2016) 489-505*
DOI: http://dx.doi.org/10.12989/sem.2016.60.3.489

Dynamic buckling of FGM viscoelastic nano-plates resting on orthotropic elastic medium based on sinusoidal shear deformation theory

A. Ghorbanpour Arani[*1,2], A. Cheraghbak[1] and R. Kolahchi[1]

[1]*Faculty of Mechanical Engineering, University of Kashan, Kashan, Iran*
[2]*Institude of Nanoscience and Nanotechnology, University of Kashan, Kashan, Iran*

(Received September 19, 2015, Revised September 8, 2016, Accepted September 9, 2016)

Abstract. Sinusoidal shear deformation theory (SSDT) is developed here for dynamic buckling of functionally graded (FG) nano-plates. The material properties of plate are assumed to vary according to power law distribution of the volume fraction of the constituents. In order to present a realistic model, the structural damping of nano-structure is considered using Kelvin-Voigt model. The surrounding elastic medium is modeled with a novel foundation namely as orthotropic visco-Pasternak medium. Size effects are incorporated based on Eringen'n nonlocal theory. Equations of motion are derived from the Hamilton's principle. The differential quadrature method (DQM) in conjunction with Bolotin method is applied for obtaining the dynamic instability region (DIR). The detailed parametric study is conducted, focusing on the combined effects of the nonlocal parameter, orthotropic visco-Pasternak foundation, power index of FG plate, structural damping and boundary conditions on the dynamic instability of system. The results are compared with those of first order shear deformation theory and higher-order shear deformation theory. It can be concluded that the proposed theory is accurate and efficient in predicting the dynamic buckling responses of system.

Keywords: dynamic buckling; FG nano-plate; SSDT; viscoelastic; orthotropic visco-Pasternak medium

1. Introduction

Functionally graded materials (FGMs) are a class of composites that have continuous variation of material properties from one surface to another and thus eliminate the stress concentration found in laminated composites. FGMs are widely used in many structural applications such as mechanics, civil engineering, aerospace, nuclear, and automotive. In company with the increase in the application of FGM in engineering structures, many computational models have been developed for predicting the response of FG plates.

Mechanical analysis on two dimensional plates was taken up by several researchers lately. Amabili (2004) worked on rectangular plates with different boundary conditions. Malekzadeh (2008), investigated tapered Mindlin plates with edges elastically restrained against rotation. Li

*Corresponding author, Professor, E-mail: aghorban@kashanu.ac.ir

http://www.techno-press.org/?journal=sem&subpage=8 ISSN: 1225-4568 (Print), 1598-6217 (Online)

and Cheng (2005) studied orthotropic plates with finite deformation and transverse shear effect. Chien and Chen (2006) worked on laminated plates on an elastic foundation.

None of the above research studies did consider nano-application. A non-local plate model was proposed by Lu, Zhang *et al*. (2007) based on Eringen's theory of non-local continuum mechanics. The bending and free vibration problems of a rectangular plate with simply supported edges are solved and the exact non-local solutions are discussed in relation to their corresponding local solutions. Narendar (2011) presented the buckling analysis of isotropic nano plates using the two variable refined plate theory and nonlocal small scale effects. It can be concluded that the present theory, which does not require shear correction factor, is not only simple but also comparable to the first-order and higher order shear deformable theory. Ghorbanpour Arani, Mosallaie Barzoki *et al*. (2011) studied Pasternak foundation effect on the axial and torsional waves propagation in the embedded double-walled carbon nanotubes (DWCNTs) using nonlocal elasticity cylindrical shell theory. The bending behaviors of the nano plate with small scale effects were investigated by Wang and Li (2012) using the nonlocal continuum theory. It can be observed that the small scale effects are obvious for bending properties of the nano plate. Transverse vibration of orthotropic DLGSs embedded in an elastic medium under thermal gradient is studied by Ghorbanpour Arani, Kolahchi *et al*. (2012) using nonlocal elasticity orthotropic plate theory. Lei, He *et al*. (2013a) developed a novel size-dependent beam model made of FGMs based on the strain gradient elasticity theory and SSDT. It is established that the present FG micro beams exhibit significant size-dependence when the thickness of the micro beam approaches to the material length scale parameter. The present model was capable of capturing both small scale effect and transverse shear deformation effects of nano beams, and does not require shear correction factors. The small scale effect on the bending of nano plates, such as grapheme sheets, embedded in two-parameter elastic medium and subjected to hydro-thermo-mechanical loading was studied by Zenkour (2013). A new higher order shear deformation theory based on trigonometric shear deformation theory was developed by Nami and Janghorban (2013). The effects of different parameters such as nonlocal parameter and aspect ratio are investigated on the deflections. In another work, Nami and Janghorban (2014) investigated the bending analysis of rectangular nano plates subjected to mechanical loading. It was established that by increasing the gradient coefficient, the deflections will decrease for both thin and thick rectangular nanoplates. Based on a nonlocal elasticity theory, Karličić (2014) structured nonlocal elasticity theory which was widely used for the analytical and computational modeling of stiffness coefficients of the elastic mediums and the number of layers on the natural frequencies and buckling load. Chakraverty and Behera (2015) studied free vibration of non-uniform embedded nanoplates based on classical plate theory in conjunction with nonlocal elasticity theory. The thermal effect on free vibration characteristics of FG size-dependent nanobeams subjected to various types of thermal loading was investigated by Ebrahimi and Salari (2015) presenting a Navier type solution and employing a semi analytical differential transform method (DTM) for the first time.

However, to date, no report has been found in the literature on dynamic stability of viscoelastic nano-plate subjected to biaxial harmonic load based on SSDT. Motivated by these considerations, in order to improve optimum design of nanostructures, we aim to present a realistic model for dynamic instability of nano-plates resting on orthotropic visco-Pasternak medium considering the viscoelastic property of the nano-plates. Nano-plates are subjected to biaxial harmonic load and modeled by SSDT.DQM is used in order to calculate the DIR of visco-nano-plates. To confirm the validity of the present research, the results are compared with those reported in the literature. The effects of the nonlocal parameter, orthotropic visco-Pasternak foundation, power index of FG

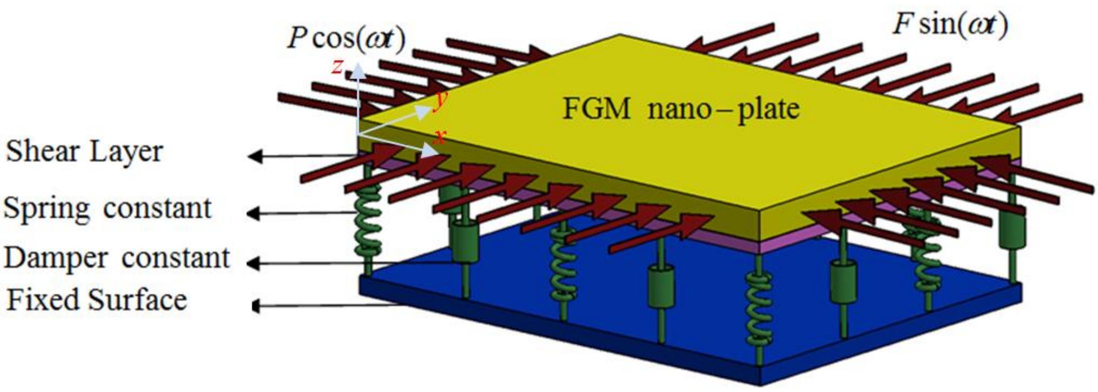

Fig. 1 Schematic of viscoelastic FG nano-plate embedded in orthotropic visco Pasternak foundation

plate, structural damping and boundary conditions on the dynamic instability of visco-system are elucidated.

2. Theoretical formulations

A schematic figure of viscoelastic FG plate resting on orthotropic visco-Pasternak foundation is shown in Fig. 1.

Based on the SSDT, the displacement field of system can be written as (Zenkour 2009)

$$\begin{aligned} U_1(X,Y,Z,T) &= U(X,Y,T) - Z\frac{\partial W_b}{\partial X} - f\frac{\partial W_s}{\partial X} \\ U_2(X,Y,Z,T) &= V(X,Y,T) - Z\frac{\partial W_b}{\partial Y} - f\frac{\partial W_s}{\partial Y} \\ U_3(X,Y,Z,T) &= W_b(X,Y,T) + W_s(X,Y,T) \end{aligned} \tag{1}$$

where

$$f = Z - \left(\frac{h}{\pi}\sin\frac{\pi Z}{h}\right) \tag{2}$$

The kinematic relations can be obtained as follows

$$\begin{Bmatrix} \varepsilon_{XX} \\ \varepsilon_{YY} \\ \varepsilon_{XY} \end{Bmatrix} = \begin{Bmatrix} \dfrac{\partial U}{\partial X} \\ \dfrac{\partial V}{\partial Y} \\ \dfrac{\partial U}{\partial Y} + \dfrac{\partial V}{\partial X} \end{Bmatrix} + Z\begin{Bmatrix} \dfrac{\partial W_b}{\partial X} \\ -\dfrac{\partial W_b}{\partial Y} \\ -2\dfrac{\partial^2 W_b}{\partial X \partial Y} \end{Bmatrix} + f\begin{Bmatrix} -\dfrac{\partial^2 W_s}{\partial X^2} \\ -\dfrac{\partial^2 W_s}{\partial Y^2} \\ -2\dfrac{\partial^2 W_s}{\partial X \partial Y} \end{Bmatrix}$$

$$\begin{Bmatrix} \gamma_{YZ} \\ \gamma_{XZ} \end{Bmatrix} = g \begin{Bmatrix} \dfrac{\partial W_s}{\partial Y} \\ \dfrac{\partial W_s}{\partial X} \end{Bmatrix} \tag{3}$$

where

$$g = 1 - \frac{df}{dZ} = \cos(\frac{\pi Z}{h}) \tag{4}$$

2.1 Constitutive equations

The material properties of FG nano-plate are assumed to vary continuously through the thickness of the plate in accordance with a power law distribution as

$$P(z) = P_M + (P_C - P_M)(\frac{1}{2} + \frac{Z}{h})^p, \tag{5}$$

where P represents the effective material property such as Young's modulus and mass density. Subscripts M and C represent the metallic and ceramic constituents, respectively; and p is the volume fraction exponent. The value of p equal to zero represents a fully ceramic nano-plate, whereas infinite p indicates a fully metallic nano-plate. Since the effects of the variation of poison's ratio on the response of FG nano-plates is very small. Based on Eringen's nonlocal theory, the linear constitutive relations of a FG nano-plate can be written as (Eringen 1983)

$$\begin{Bmatrix} \sigma_{XX}^{nl} \\ \sigma_{YY}^{nl} \\ \sigma_{XY}^{nl} \\ \sigma_{YZ}^{nl} \\ \sigma_{XZ}^{nl} \end{Bmatrix} - (e_0 a)^2 \nabla^2 \begin{Bmatrix} \sigma_{XX}^{l} \\ \sigma_{YY}^{l} \\ \sigma_{XY}^{l} \\ \sigma_{YZ}^{l} \\ \sigma_{XZ}^{l} \end{Bmatrix} = \begin{bmatrix} C_{11} & C_{12} & 0 & 0 & 0 \\ C_{21} & C_{22} & 0 & 0 & 0 \\ 0 & 0 & C_{44} & 0 & 0 \\ 0 & 0 & 0 & C_{55} & 0 \\ 0 & 0 & 0 & 0 & C_{66} \end{bmatrix} \begin{Bmatrix} \varepsilon_{XX} \\ \varepsilon_{YY} \\ \varepsilon_{XY} \\ \gamma_{YZ} \\ \gamma_{XZ} \end{Bmatrix} \tag{6}$$

where C_{11} are elastic constants and e_0a represents the size effects. All materials exhibit some viscoelastic response.According to Kelvin-Voigt (Lei, Adhikari *et al*. 2013b) at real life, nano structure mechanical properties depend on the time variation. This model represents,as the stress is released, the material gradually relaxes to its undeformed state.By considering this model,we have

$$C_{ij} = C_{ij}\left(1 + g\frac{\partial}{\partial t}\right), \tag{7}$$

where g is structural damping constant.

2.2 Equations of motion

Hamilton's principle is used herein to derive the equations of motion. The principle can be stated in analytical form as

$$0=\int_0^t\left(\delta U+\delta W-\delta K\right)dt, \tag{8}$$

where δU is the variation of potential energy; δW is the variation of external works; and δK is the variation of kinetic energy. The variation of strain energy of the FGM viscoelastic nano-plate is calculated by

$$\begin{aligned}\partial U &= \int_V (\sigma_{XX}\partial\varepsilon_{XX}+\sigma_{YY}\partial\varepsilon_{YY}+\sigma_{XY}\partial\gamma_{XY}+\sigma_{YZ}\partial\gamma_{YZ}+\sigma_{XZ}\partial\gamma_{XZ})dAdZ\\ &=\int_V \Bigg\{N_x\frac{\partial\delta U}{\partial X}-M_x^b\frac{\partial^2\delta W_b}{\partial X^2}-M_x^s\frac{\partial^2\delta W_s}{\partial X^2}+N_y\frac{\partial\delta U}{\partial Y}-M_y^b\frac{\partial^2\delta V_b}{\partial Y^2}-M_y^s\frac{\partial^2\delta W_s}{\partial Y^2}\\ &+N_{xy}\left(\frac{\partial\delta U}{\partial Y}+\frac{\partial\delta U}{\partial X}\right)-2M_{xy}^b\frac{\partial^2\delta W_b}{\partial X\partial Y}-2M_{xy}^s\frac{\partial^2\delta W_s}{\partial X\partial Y}+Q_{yz}\frac{\partial\delta W_s}{\partial Y}+Q_{xz}\frac{\partial\delta W_x}{\partial X}\Bigg\}dA\end{aligned} \tag{9}$$

where N, M, and Q are the stress resultants which may be defined as

$$N_I,M_i^b,M_i^s\_=\int_{-\frac{h}{2}}^{\frac{h}{2}}(1,Z,f)\sigma_i dZ,\quad (i=x,y,xy) \tag{10}$$

$$Q_i=\int_{-\frac{h}{2}}^{\frac{n}{2}}h\sigma_i dZ,\quad i(xy,yz) \tag{11}$$

The variation of external works can be expressed as

$$\delta W=-\int_A q\delta U_3 dA \tag{12}$$

where q is transverse loads due to orthotropic elastic foundation which is (2012)

$$\begin{aligned}q&=kU_3-G_\xi\left(\cos^2\theta U_{3,xx}+2\cos\theta\sin\theta U_{3,yx}+\sin^2\theta U_{3,yy}\right)\\ &-G_\eta\left(\sin^2\theta U_{3,xx}-2\sin\theta\cos\theta U_{3,yx}+\cos^2\theta U_{3,yy}\right),\end{aligned} \tag{13}$$

where angle θ describes the local ξ direction of orthotropic foundation with respect to the global x-axis of the plate; k, G_ξ and G_η are Winkler foundation parameter, shear foundation parameters in ξ and η directions, respectively.

The variation of kinetic energy of the nano-plate can be written as

$$\begin{aligned}\delta K&=\int_V(\dot U_1\delta\dot U_1+\dot U_2\delta\dot U_2+\dot U_3\delta\dot U_3)\rho(z)dAdz\\ &=\int_A\{I_O[\dot U\partial\dot U+\dot V\partial\dot V+(\dot W_b+\dot W_s)\partial(\dot W_b+\dot W_s)]\\ &-I_1\left(\dot U\frac{\partial\delta\dot W_b}{\partial X}+\delta\dot U\frac{\partial\delta\dot W_s}{\partial X}+\dot V\frac{\partial\delta\dot W_s}{\partial Y}+\delta\dot V\frac{\partial\dot W_s}{\partial Y}+I_2\right)\\ &-J_1\left(\dot U\frac{\partial\delta\dot W_s}{\partial X}+\delta\dot U\frac{\partial\dot W_s}{\partial X}+\dot V\frac{\partial\delta\dot W_s}{\partial Y}+\delta\dot V\frac{\partial\dot W_s}{\partial Y}+I_2\left(\frac{\partial\dot W_b}{\partial X}\frac{\partial\delta\dot W_b}{\partial X}+\frac{\partial\delta\dot W_b}{\partial Y}\frac{\partial\dot W_b}{\partial Y}\right)\right.\end{aligned}$$

$$
\begin{aligned}
&+K_2\left(\frac{\partial \dot{W}_s}{\partial X}\frac{\partial \delta \dot{W}_s}{\partial X}+\frac{\partial \delta \dot{W}_s}{\partial Y}\frac{\partial \dot{W}_s}{\partial Y}\right)\\
&\left.+J_2\left(\frac{\partial \dot{W}_b}{\partial X}\frac{\partial \delta \dot{W}_s}{\partial X}+\frac{\partial \delta \dot{W}_b}{\partial X}\frac{\partial \dot{W}_s}{\partial X}+\frac{\partial \dot{W}_b}{\partial Y}\frac{\partial \delta \dot{W}_s}{\partial Y}+\frac{\partial \delta \dot{W}_b}{\partial Y}\frac{\partial \dot{W}_s}{\partial Y}\right)\right)\Bigg\}dA
\end{aligned}
\tag{14}
$$

where the mass inertias can be defined as

$$
(I_0, I_1, I_2, J_1, J_2, K_2)=\int_{-\frac{h}{2}}^{\frac{h}{2}}(1, Z, f, Zf, Z^2, f^2)\rho(z)dz \tag{15}
$$

Substituting the expressions for δU, δW, and δK from Eqs. (9)-(14) into Eq. (8) yields the following motion equations

$$
\delta U:\frac{\partial N_x}{\partial X}+\frac{\partial N_{xy}}{\partial Y}=I_0\ddot{u}-I_1\frac{\partial \ddot{w}_b}{\partial X}-J_1\frac{\partial \ddot{w}_s}{\partial X} \tag{16a}
$$

$$
\delta V:\frac{\partial N_{xy}}{\partial X}+\frac{\partial N_y}{\partial Y}=I_0\ddot{v}-I_1\frac{\partial \ddot{w}_b}{\partial Y}-J_1\frac{\partial \ddot{w}_s}{\partial Y} \tag{16b}
$$

$$
\begin{aligned}
&\delta W_s:\frac{\partial^2 M_x^s}{\partial X^2}+2\frac{\partial^2 M_{xy}^s}{\partial X\partial Y}+\frac{\partial^2 M_y^s}{\partial Y^2}+\frac{\partial Q_{xz}}{\partial X}+\frac{\partial Q_{yz}}{\partial Y}+q\\
&-I_0(\ddot{W}_b+\ddot{W}_s)+J_1\left(\frac{\partial \ddot{U}}{\partial X}+\frac{\partial \ddot{V}}{\partial Y}\right)-J_2\nabla^2\ddot{W}_b-K_2\nabla^2\ddot{W}_s
\end{aligned}
\tag{16c}
$$

$$
\delta W_b:\frac{\partial^2 M_x^b}{\partial X^2}+2\frac{\partial^2 M_{xy}^b}{\partial X\partial Y}+\frac{\partial^2 M_y^b}{\partial Y^2}+q=I_0(\ddot{W}_b+\ddot{W}_s)+I_1\left(\frac{\partial \ddot{U}}{\partial X}+\frac{\partial \ddot{V}}{\partial Y}\right)-I_2\nabla^2\ddot{W}_b-J_2\nabla^2\ddot{W}_s \tag{16d}
$$

By substituting Eqs. (6) and (7) into Eqs. (10) and (11) the stress resultants are obtained as

$$
\begin{aligned}
N_{XX}=&\int_{\frac{-h}{2}}^{\frac{h}{2}}(C_{11}\varepsilon_{XX}+C_{12}\varepsilon_{YY})dz=\left\{[A_{10}(Z)+A_{20}(Z)](\frac{\partial U}{\partial X})\right\}-\left\{[A_{11}(Z)+A_{21}(Z)](\frac{\partial^2 W_b}{\partial X^2})\right\}-\\
&\left\{[A_{11}(Z)+A_{21}(Z)](\frac{\partial^2 W_s}{\partial X^2})\right\}+\left\{(\frac{h}{\pi}\sin\frac{\pi z}{h})[A_{10}(Z)+A_{20}(Z)](\frac{\partial^2 W_s}{\partial X^2})\right\}+\left\{[A_{30}(Z)+A_{40}(Z)](\frac{\partial V}{\partial Y})\right\}\\
&-\left\{[A_{31}(Z)+A_{41}(Z)](\frac{\partial^2 W_b}{\partial Y^2})\right\}-\left\{[A_{31}(Z)+A_{41}(Z)](\frac{\partial^2 W_S}{\partial Y^2})\right\}+\left\{(\frac{h}{\pi}\sin\frac{\pi z}{h})[A_{30}(Z)+A_{40}(Z)](\frac{\partial^2 W_s}{\partial Y^2})\right\}
\end{aligned}
$$

$$
\begin{aligned}
N_{YY}=&\int_{\frac{-h}{2}}^{\frac{h}{2}}(C_{21}\varepsilon_{XX}+C_{22}\varepsilon_{YY})dz=\left\{[A_{70}(Z)+A_{80}(Z)](\frac{\partial V}{\partial Y})\right\}-\left\{[A_{71}(Z)+A_{81}(Z)](\frac{\partial^2 W_b}{\partial Y^2})\right\}-\\
&\left\{[A_{71}(Z)+A_{81}(Z)](\frac{\partial^2 W_s}{\partial Y^2})\right\}+\left\{(\frac{h}{\pi}\sin\frac{\pi z}{h})[A_{70}(Z)+A_{80}(Z)](\frac{\partial^2 W_s}{\partial Y^2})\right\}+\left\{[A_{50}(Z)+A_{60}(Z)](\frac{\partial U}{\partial X})\right\}
\end{aligned}
$$

$$-\left\{\left[A_{51}(Z)+A_{61}(Z)\right](\frac{\partial^2 W_b}{\partial X^2})\right\}-\left\{\left[A_{51}(Z)+A_{61}(Z)\right](\frac{\partial^2 W_S}{\partial X^2})\right\}+\left\{(\frac{h}{\pi}\sin\frac{\pi z}{h})\left[A_{50}(Z)+A_{60}(Z)\right](\frac{\partial^2 W_s}{\partial X^2})\right\}$$

$$N_{XY}=\int_{\frac{-h}{2}}^{\frac{h}{2}}(C_{66}\varepsilon_{XY})dz=\left\{\left[A_{130}(Z)+A_{140}(Z)\right](\frac{\partial U}{\partial Y})\right\}-\left\{\left[A_{130}(Z)+A_{140}(Z)\right](\frac{\partial V}{\partial X})\right\}-$$

$$-2\left\{\left[A_{131}(Z)+A_{141}(Z)\right](\frac{\partial^2 W_s}{\partial X\partial Y})\right\}+2\left\{(\frac{h}{\pi}\sin\frac{\pi z}{h})\left[A_{130}(Z)+A_{140}(Z)\right](\frac{\partial^2 W_s}{\partial X\partial Y})\right\}-2\left\{\left[A_{130}(Z)+A_{140}(Z)\right](\frac{\partial^2 W_s}{\partial X\partial Y})\right\} \tag{17}$$

$$Q_{XZ}=\int_{\frac{-h}{2}}^{\frac{h}{2}}(gC_{55}\gamma_{XZ})dz=\left\{\left[A_{110}(Z)+A_{120}(Z)\right](\cos\frac{\pi z}{h})^2(\frac{\partial W_s}{\partial X})\right\}$$

$$Q_{YZ}=\int_{\frac{-h}{2}}^{\frac{h}{2}}(gC_{44}\gamma_{YZ})dz=\left\{\left[A_{90}(Z)+A_{100}(Z)\right](\cos\frac{\pi z}{h})^2(\frac{\partial W_s}{\partial Y})\right\}$$

$$M^b_{XX}=\int_{\frac{-h}{2}}^{\frac{h}{2}}(C_{11}\varepsilon_{XX}+C_{12}\varepsilon_{YY})ZdZ=\left\{\left[A_{11}(Z)+A_{21}(Z)\right](\frac{\partial U}{\partial X})\right\}-\left\{\left[A_{12}(Z)+A_{22}(Z)\right](\frac{\partial^2 W_b}{\partial X^2})\right\}$$

$$-\left\{\left[A_{12}(Z)+A_{22}(Z)\right](\frac{\partial^2 W_s}{\partial X^2})\right\}+\left\{(\frac{h}{\pi}\sin\frac{\pi Z}{h})\left[A_{11}(Z)+A_{21}(Z)\right](\frac{\partial^2 W_s}{\partial X^2})\right\}+\left\{\left[A_{31}(Z)+A_{41}(Z)\right](\frac{\partial V}{\partial Y})\right\}$$

$$-\left\{\left[A_{32}(Z)+A_{42}(Z)\right](\frac{\partial^2 W_b}{\partial Y^2})\right\}-\left\{\left[A_{32}(Z)+A_{42}(Z)\right](\frac{\partial^2 W_s}{\partial Y^2})\right\}+\left\{(\frac{h}{\pi}\sin\frac{\pi Z}{h})\left[A_{31}(Z)+A_{41}(Z)\right](\frac{\partial^2 W_s}{\partial Y^2})\right\},$$

$$M^b_{YY}=\int_{\frac{-h}{2}}^{\frac{h}{2}}(C_{21}\varepsilon_{XX}+C_{22}\varepsilon_{YY})ZdZ=\left\{\left[A_{71}(Z)+A_{81}(Z)\right](\frac{\partial V}{\partial Y})\right\}-\left\{\left[A_{72}(Z)+A_{82}(Z)\right](\frac{\partial^2 W_b}{\partial Y^2})\right\} \tag{18}$$

$$-\left\{\left[A_{72}(Z)+A_{82}(Z)\right](\frac{\partial^2 W_s}{\partial Y^2})\right\}+\left\{(\frac{h}{\pi}\sin\frac{\pi Z}{h})\left[A_{71}(Z)+A_{81}(Z)\right](\frac{\partial^2 W_s}{\partial Y^2})\right\}+\left\{\left[A_{51}(Z)+A_{61}(Z)\right](\frac{\partial U}{\partial X})\right\}$$

$$-\left\{\left[A_{52}(Z)+A_{62}(Z)\right](\frac{\partial^2 W_b}{\partial X^2})\right\}-\left\{\left[A_{52}(Z)+A_{62}(Z)\right](\frac{\partial^2 W_s}{\partial X^2})\right\}+\left\{(\frac{h}{\pi}\sin\frac{\pi Z}{h})\left[A_{51}(Z)+A_{61}(Z)\right](\frac{\partial^2 W_s}{\partial X^2})\right\},$$

$$M^b_{XY}=\int_{\frac{-h}{2}}^{\frac{h}{2}}(2C_{66}\varepsilon_{XY})ZdZ=\left\{\left[A_{131}(Z)+A_{141}(Z)\right](\frac{\partial U}{\partial Y})\right\}+\left\{\left[A_{131}(Z)+A_{141}(Z)\right](\frac{\partial V}{\partial X})\right\}$$

$$-2\left\{\left[A_{132}(Z)+A_{142}(Z)\right](\frac{\partial^2 W_s}{\partial X\partial Y})\right\}+2\left\{(\frac{h}{\pi}\sin\frac{\pi Z}{h})\left[A_{131}(Z)+A_{141}(Z)\right](\frac{\partial^2 W_s}{\partial X\partial Y})\right\}-2\left\{\left[A_{132}(Z)+A_{142}(Z)\right](\frac{\partial^2 W_b}{\partial X\partial Y})\right\},$$

$$M^S_{XX}=\int_{\frac{-h}{2}}^{\frac{h}{2}}(C_{11}\varepsilon_{XX}+C_{21}\varepsilon_{YY})fdZ=\left\{\left[A_{10f}(Z)+A_{20f}(Z)\right](\frac{\partial U}{\partial X})\right\}-\left\{\left[A_{11f}(Z)+A_{21f}(Z)\right](\frac{\partial^2 W_b}{\partial X^2})\right\}$$

$$-\left\{\left[A_{11f}(Z)+A_{21f}(Z)\right](\frac{\partial^2 W_s}{\partial X^2})\right\}+\left\{(\frac{h}{\pi}\sin\frac{\pi Z}{h})\left[A_{10f}(Z)+A_{20f}(z)\right](\frac{\partial^2 W_s}{\partial X^2})\right\}+\left\{\left[A_{30f}(Z)+A_{40f}(Z)\right](\frac{\partial V}{\partial Y})\right\}$$

$$-\left\{\left[A_{31f}(Z)+A_{41f}(Z)\right](\frac{\partial^2 W_b}{\partial Y^2})\right\}-\left\{\left[A_{31f}(Z)+A_{41f}(Z)\right](\frac{\partial^2 W_S}{\partial Y^2})\right\}+\left\{(\frac{h}{\pi}\sin\frac{\pi Z}{h})\left[A_{30f}(Z)+A_{40f}(Z)\right](\frac{\partial^2 W_s}{\partial Y^2})\right\},$$

$$M^S_{YY}=\int_{\frac{-h}{2}}^{\frac{h}{2}}(C_{21}\varepsilon_{XX}+C_{22}\varepsilon_{YY})fdZ=\left\{\left[A_{50f}(Z)+A_{60f}(Z)\right](\frac{\partial U}{\partial X})\right\}-\left\{\left[A_{51f}(Z)+A_{61f}(Z)\right](\frac{\partial^2 W_b}{\partial X^2})\right\}$$

$$-\left\{\left[A_{51f}(Z)+A_{61f}(z)\right](\frac{\partial^2 W_s}{\partial X^2})\right\}+\left\{(\frac{h}{\pi}\sin\frac{\pi Z}{h})\left[A_{50f}(z)+A_{60f}(Z)\right](\frac{\partial^2 W_s}{\partial X^2})\right\}+\left\{\left[A_{70f}(Z)+A_{80f}(Z)\right](\frac{\partial V}{\partial Y})\right\}$$

$$-\left\{\left[A_{71f}(Z)+A_{81f}(Z)\right](\frac{\partial^2 W_b}{\partial Y^2})\right\}-\left\{\left[A_{71f}(Z)+A_{81f}(Z)\right](\frac{\partial^2 W_s}{\partial Y^2})\right\}+\left\{(\frac{h}{\pi}\sin\frac{\pi Z}{h})\left[A_{70f}(Z)+A_{80f}(Z)\right](\frac{\partial^2 W_s}{\partial Y^2})\right\},$$

$$M_{XY}^{S}=\int_{\frac{-h}{2}}^{\frac{h}{2}}2(C_{66}\varepsilon_{XY})\,f dZ=2\left\{\left[A_{130f}(Z)+A_{140f}(Z)\right](\frac{\partial U}{\partial Y})\right\}+2\left\{\left[A_{130f}(Z)+A_{140f}(Z)\right](\frac{\partial V}{\partial X})\right\} \tag{19}$$

$$-2\left\{\left[A_{131f}(Z)+A_{141f}(Z)\right](\frac{\partial^2 W_s}{\partial X\partial Y})\right\}-2\left\{\left[A_{131f}(Z)+A_{141f}(Z)\right](\frac{\partial^2 W_b}{\partial X\partial Y})\right\}+2\left\{(\frac{h}{\pi}\sin\frac{\pi Z}{h})\left[A_{131f}(z)+A_{141f}(Z)\right](\frac{\partial^2 W_b}{\partial X\partial Y})\right\},$$

where

$$A_{1K}=\int_{\frac{-h}{2}}^{\frac{h}{2}}C_{11M}Z^K dZ \qquad K=0,1,2 \qquad A_{1Kf}=\int_{\frac{-h}{2}}^{\frac{h}{2}}C_{11M}Z^K f dZ \qquad K=0,1$$

$$A_{1Kff}=\int_{\frac{-h}{2}}^{\frac{h}{2}}C_{11M}Z^K f^2 dZ, \qquad A_{2K}=\int_{\frac{-h}{2}}^{\frac{h}{2}}(C_{11C}-C_{11M})(\frac{1}{2}+\frac{Z}{h})^p Z^K dZ$$

$$A_{2Kf}=\int_{\frac{-h}{2}}^{\frac{h}{2}}(C_{11C}-C_{11M})(\frac{1}{2}+\frac{Z}{h})^p Z^K f dZ, \qquad A_{2Kff}=\int_{\frac{-h}{2}}^{\frac{h}{2}}(C_{11C}-C_{11M})(\frac{1}{2}+\frac{Z}{h})^p Z^K f^2 dZ$$

$$A_{3K}=\int_{\frac{-h}{2}}^{\frac{h}{2}}C_{12M}Z^K dZ, \qquad A_{3K}=\int_{\frac{-h}{2}}^{\frac{h}{2}}C_{12M}Z^K dZ$$

$$A_{3K}=\int_{\frac{-h}{2}}^{\frac{h}{2}}C_{12M}Z^K dZ, \quad A_{3Kf}=\int_{\frac{-h}{2}}^{\frac{h}{2}}C_{12M}Z^K fdZ, \quad A_{3Kff}=\int_{\frac{-h}{2}}^{\frac{h}{2}}C_{12M}Z^K f^2 dZ, \quad A_{4K}=\int_{\frac{-h}{2}}^{\frac{h}{2}}(C_{12C}-C_{12M})(\frac{1}{2}+\frac{Z}{h})^P Z^K dZ,$$

$$A_{4Kf}=\int_{\frac{-h}{2}}^{\frac{h}{2}}(C_{12C}-C_{12M})(\frac{1}{2}+\frac{Z}{h})^P Z^K fdZ, \quad A_{4Kff}=\int_{\frac{-h}{2}}^{\frac{h}{2}}(C_{12C}-C_{12M})(\frac{1}{2}+\frac{Z}{h})^P Z^K f^2 dZ$$

$$A_{5K}=\int_{\frac{-h}{2}}^{\frac{h}{2}}C_{21M}Z^K dZ, \quad A_{5Kf}=\int_{\frac{-h}{2}}^{\frac{h}{2}}C_{21M}Z^K fdZ, \quad A_{5Kff}=\int_{\frac{-h}{2}}^{\frac{h}{2}}C_{21M}Z^K f^2 dZ, \quad A_{6K}=\int_{\frac{-h}{2}}^{\frac{h}{2}}(C_{21C}-C_{21M})(\frac{1}{2}+\frac{Z}{h})^P Z^K dZ,$$

$$A_{6Kf}=\int_{\frac{-h}{2}}^{\frac{h}{2}}(C_{21C}-C_{21M})(\frac{1}{2}+\frac{Z}{h})^P Z^K fdZ, \quad A_{6Kff}=\int_{\frac{-h}{2}}^{\frac{h}{2}}(C_{21C}-C_{21M})(\frac{1}{2}+\frac{Z}{h})^P Z^K f^2 dZ$$

$$A_{7K}=\int_{\frac{-h}{2}}^{\frac{h}{2}}C_{22M}Z^K dZ, \quad A_{7Kf}=\int_{\frac{-h}{2}}^{\frac{h}{2}}C_{22M}Z^K fdZ, \quad A_{7Kff}=\int_{\frac{-h}{2}}^{\frac{h}{2}}C_{22M}Z^K f^2 dZ, \quad A_{8K}=\int_{\frac{-h}{2}}^{\frac{h}{2}}(C_{22C}-C_{22M})(\frac{1}{2}+\frac{Z}{h})^P Z^K dZ,$$

$$A_{8Kf}=\int_{\frac{-h}{2}}^{\frac{h}{2}}(C_{22C}-C_{22M})(\frac{1}{2}+\frac{Z}{h})^P Z^K fdZ, \quad A_{8Kff}=\int_{\frac{-h}{2}}^{\frac{h}{2}}(C_{22C}-C_{22M})(\frac{1}{2}+\frac{Z}{h})^P Z^K f^2 dZ$$

$$A_{9K}=\int_{-h/2}^{h/2}C_{44M}Z^{K}dZ,\quad A_{9Kf}=\int_{-h/2}^{h/2}C_{44M}Z^{K}fdZ,\quad A_{9Kff}=\int_{-h/2}^{h/2}C_{44M}Z^{K}f^{2}dZ,\quad A_{10K}=\int_{-h/2}^{h/2}(C_{44C}-C_{44M})(\frac{1}{2}+\frac{Z}{h})^{P}Z^{K}dZ,$$

$$A_{10Kf}=\int_{-h/2}^{h/2}(C_{44C}-C_{44M})(\frac{1}{2}+\frac{Z}{h})^{P}Z^{K}fdZ,\quad A_{10Kff}=\int_{-h/2}^{h/2}(C_{44C}-C_{44M})(\frac{1}{2}+\frac{Z}{h})^{P}Z^{K}f^{2}dZ$$

$$A_{11K}==\int_{-h/2}^{h/2}C_{55M}Z^{K}dZ,\quad A_{11Kf}=\int_{-h/2}^{h/2}C_{55M}Z^{K}fdZ,\quad A_{11Kff}=\int_{-h/2}^{h/2}C_{55M}Z^{K}f^{2}dZ,$$

$$A_{10Kff}=\int_{-h/2}^{h/2}(C_{44C}-C_{44M})(\frac{1}{2}+\frac{Z}{h})^{P}Z^{K}f^{2}dZ,\quad A_{11K}=\int_{-h/2}^{h/2}C_{55M}Z^{K}dZ,\quad A_{11Kf}=\int_{-h/2}^{h/2}C_{55M}Z^{K}fdZ,$$

$$A_{11Kff}=\int_{-h/2}^{h/2}C_{55M}Z^{K}f^{2}dZ,\quad A_{12K}=\int_{-h/2}^{h/2}(C_{55C}-C_{55M})(\frac{1}{2}+\frac{Z}{h})^{P}Z^{K}dZ,$$

$$A_{12Kf}=\int_{-h/2}^{h/2}(C_{55C}-C_{55M})(\frac{1}{2}+\frac{Z}{h})^{P}Z^{K}fdZ,\quad A_{12Kff}=\int_{-h/2}^{h/2}(C_{55C}-C_{55M})(\frac{1}{2}+\frac{Z}{h})^{P}Z^{K}f^{2}dZ$$

$$A_{13K}=\int_{-h/2}^{h/2}C_{66M}Z^{K}dZ,\quad A_{13Kf}=\int_{-h/2}^{h/2}C_{66M}Z^{K}fdZ,\quad A_{13Kff}=\int_{-h/2}^{h/2}C_{66M}Z^{K}f^{2}dZ, \tag{20}$$

$$A_{14K}=\int_{-h/2}^{h/2}(C_{66C}-C_{66M})(\frac{1}{2}+\frac{Z}{h})^{P}Z^{K}dZ,\quad A_{14Kf}=\int_{-h/2}^{h/2}(C_{66C}-C_{66M})(\frac{1}{2}+\frac{Z}{h})^{P}Z^{K}fdZ,$$

$$A_{14Kff}=\int_{-h/2}^{h/2}(C_{66C}-C_{66M})(\frac{1}{2}+\frac{Z}{h})^{P}Z^{K}f^{2}d,$$

By substituting Eqs. (17)-(19)into Eq. (16), the equations of motion can be expressed as

$$\begin{aligned}
&(A_{10}+A_{20})(\frac{\partial^2}{\partial X^2}U)-(A_{11}+A_{21})(\frac{\partial^3}{\partial X^3}W_b)+(A_{11}+A_{21})(\frac{\partial^3}{\partial X^3}W_s)+(A_{11F}+A_{21F})(\frac{\partial^3}{\partial X^3}W_s)\\
&+(A_{30}+A_{40})(\frac{\partial^2}{\partial X\partial Y}V)-(A_{31}+A_{41})(\frac{\partial^3}{\partial X\partial Y^2}W_b)-(A_{31}+A_{41})(\frac{\partial^3}{\partial X\partial Y^2}W_s)\\
&+(A_{31F}+A_{41F})(\frac{\partial^3}{\partial X\partial Y^2}W_s)+(A_{130}+A_{140})(\frac{\partial^2}{\partial Y^2}U)+(A_{130}+A_{140})(\frac{\partial^2}{\partial X\partial Y}V)\\
&-2(A_{131}+A_{141})(\frac{\partial^3}{\partial X\partial Y^2}W_s)+2(A_{131F}+A_{141F})(\frac{\partial^3}{\partial X\partial Y^2}W_s)-2(A_{131}+A_{141})(\frac{\partial^3}{\partial X\partial Y^2}W_b)\\
&-(1-(e_0a)^2\nabla^2)\left[I_0(\frac{\partial^2}{\partial T^2}U)+I_1(\frac{\partial^3}{\partial X\partial T^2}W_b)+J_1(\frac{\partial^3}{\partial X\partial T^2}W_s)\right]=0,
\end{aligned} \tag{21}$$

$$
\begin{aligned}
&(A_{130}+A_{140})(\frac{\partial^2}{\partial X\partial Y}U)+(A_{130}+A_{140})(\frac{\partial^2}{\partial X^2}V)-2(A_{131}+A_{141})(\frac{\partial^3}{\partial Y\partial X^2}W_s)+2(A_{131F}+A_{141F})(\frac{\partial^3}{\partial Y\partial X^2}W_s)\\
&-2(A_{131}+A_{141})(\frac{\partial^3}{\partial Y\partial X^2}W_b)+(A_{70}+A_{80})(\frac{\partial^2}{\partial Y^2}V)-(A_{71}+A_{81})(\frac{\partial^3}{\partial Y^3}W_b)-(A_{71}+A_{81})(\frac{\partial^3}{\partial Y^3}W_s)\\
&+(A_{71F}+A_{81F})(\frac{\partial^3}{\partial Y\partial X^2}W_s)+(A_{50}+A_{60})(\frac{\partial^2}{\partial X\partial Y}U)-(A_{51}+A_{61})(\frac{\partial^3}{\partial Y\partial X^2}W_s)+(A_{51F}+A_{61F})(\frac{\partial^3}{\partial Y\partial X^2}W_s)\\
&+(1-(e_0a)^2\nabla^2)\left[-I_0(\frac{\partial^2}{\partial T^2}V)+I_1.\frac{\partial^3}{\partial Y\partial T^2}W_b+J_1.\frac{\partial^3}{\partial Y\partial T^2}W_s\right]=0,
\end{aligned}
\tag{22}
$$

$$
\begin{aligned}
&-(A_{12}+A_{22}).(\frac{\partial^4}{\partial X^4}W_s)+2((A_{131}+A_{141}).(\frac{\partial^3}{\partial Y^2\partial X}U)+(A_{71}+A_{81}).(\frac{\partial^3}{\partial Y^3}V)+(A_{31}+A_{41}).(\frac{\partial^3}{\partial X^2\partial Y}V)\\
&+4.(FF.(A_{131}+A_{141}).(\frac{\partial^4}{\partial Y^2\partial X^2}W_s)+(FF.(A_{71}+A_{81}).(\frac{\partial^4}{\partial Y^2\partial X^2}W_s))+(A_{51}+A_{61})(\frac{\partial^3}{\partial Y^2\partial X}U)+\\
&2((A_{131}+A_{141})\frac{\partial^3}{\partial X^2\partial Y}V)-(A_{32}+A_{42}).(\frac{\partial^4}{\partial Y^2\partial X^2}W_s)-(A_{72}+A_{82}).(\frac{\partial^4}{\partial Y^4}W_s)-4(A_{132}+A_{142}).(\frac{\partial^4}{\partial Y^2\partial X^2}W_s)\\
&-4(A_{132}+A_{142}).(\frac{\partial^4}{\partial Y^2\partial X^2}W_b)+FF(A_{31}+A_{41}).(\frac{\partial^4}{\partial Y^2\partial X^2}W_s)-(A_{52}+A_{62}).(\frac{\partial^4}{\partial Y^2\partial X^2}W_b)+(\frac{\partial^2}{\partial Y^2}W_b+\frac{\partial^2}{\partial Y^2}W_s)\\
&-(A_{12}+A_{22}).(\frac{\partial^4}{\partial X^4}W_s)--(A_{32}+A_{42}).(\frac{\partial^4}{\partial Y^2\partial X^2}W_b)+FF(A_{11}+A_{21}).(\frac{\partial^4}{\partial X^4}W_s)-(A_{52}+A_{62}).(\frac{\partial^4}{\partial Y^2\partial X^2}W_s)\\
&-(A_{72}+A_{82}).(\frac{\partial^4}{\partial Y^4}W_b)+(A_{11}+A_{21}).(\frac{\partial^3}{\partial X^3}U)+(1-(e_0a)^2\nabla^2)\Big[(F\cos(\Omega T)(\frac{\partial^2}{\partial X^2}W_b+\frac{\partial^2}{\partial X^2}W_s\\
&+P\cos(\omega T)(\frac{\partial^2}{\partial Y^2}W_b+\frac{\partial^2}{\partial Y^2}W_s)+k(W_b+W_s)-G_\xi\left(\cos^2\theta(W_b+W_s)_{,xx}+2\cos\theta\sin\theta(W_b+W_s)_{,yx}+\sin^2\theta(W_b+W_s)_{,yy}\right)\\
&-G_\eta\left(\sin^2\theta(W_b+W_s)_{,xx}-2\sin\theta\cos\theta(W_b+W_s)_{,yx}+\cos^2\theta(W_b+W_s)_{,yy}\right)+I_2.(\frac{\partial^4}{\partial T^2\partial X^2}W_b+\frac{\partial^4}{\partial T^2\partial Y^2}W_b)\\
&+J_2.(\frac{\partial^4}{\partial T^2\partial X^2}W_s+\frac{\partial^4}{\partial T^2\partial Y^2}W_s)-I_0.(\frac{\partial^2}{\partial T^2}W_b+\frac{\partial^2}{\partial T^2}W_s)-I_1.((\frac{\partial^3}{\partial T^2\partial X}U(+\frac{\partial^3}{\partial T^2\partial X}V))\Big]=0,
\end{aligned}
\tag{23}
$$

$$
\begin{aligned}
&4((A_{130F}+A_{140F})(\frac{\partial}{\partial X}\frac{\partial^2}{\partial Y^2}U)+(A_{110}+A_{120})(\cos(\frac{\pi Z}{h})^2)(\frac{\partial^2}{\partial X^2}W_s)-(A_{31F}+A_{41F})(\frac{\partial^4}{\partial Y^2\partial X^2}W_b)-\\
&4((A_{131F}+A_{141F})(\frac{\partial^4}{\partial Y^2\partial X^2}W_s)-(A_{51F}+A_{61F})(\frac{\partial^4}{\partial Y^2\partial X^2}W_b)-4((A_{131F}+A_{141F})(\frac{\partial^4}{\partial Y^2\partial X^2}W_b)\\
&-(A_{71F}+A_{81F})(\frac{\partial^4}{\partial Y^4}W_s)+FF(A_{10F}+A_{20F})(\frac{\partial^4}{\partial X^4}W_s)-((A_{31F}+A_{41F})(\frac{\partial^4}{\partial Y^2\partial X^2}W_s)+\\
&((A_{30F}+A_{40F})(\frac{\partial}{\partial Y}\frac{\partial^2}{\partial X^2}V)+FF(A_{70F}+A_{80F})(\frac{\partial^4}{\partial Y^4}W_s)-(A_{11F}+A_{21F})(\frac{\partial^4}{\partial X^4}W_s)\\
&+FF(A_{50F}+A_{60F})(\frac{\partial^4}{\partial Y^2\partial X^2}W_s)-(A_{51F}+A_{61F})(\frac{\partial^4}{\partial Y^2\partial X^2}W_s)+(A_{50F}+A_{60F})(\frac{\partial^3}{\partial Y^2\partial X}U)\\
&+2(A_{130F}+A_{140F})(\frac{\partial^3}{\partial X^2\partial Y}V)+4.(FF(A_{130F}+A_{140F}).(\frac{\partial^4}{\partial Y^2\partial X^2}W_s)+(A_{70F}+A_{80F})(\frac{\partial^3}{\partial Y^3}V)\\
&+K_2J(\frac{\partial^4}{\partial X^2\partial T^2}W_b+\frac{\partial^4}{\partial Y^2\partial T^2}W_b)-(A_{11F}+A_{21F})(\frac{\partial^4}{\partial X^4}W_b)+(A_{10F}+A_{20F})(\frac{\partial^3}{\partial X^3}U)-(A_{71F}+A_{81F})(\frac{\partial^4}{\partial Y^4}W_b)\\
&+FF(A_{30F}+A_{40F})(\frac{\partial^4}{\partial Y^2\partial X^2}W_s)+(A_{90}+A_{100})(\cos(\frac{\pi Z}{h})^2)(\frac{\partial^2}{\partial Y^2}W_s)+(1-(e_0a)^2\nabla^2)\big[+k(W_b+W_s)\\
&-G_\xi\left(\cos^2\theta(W_b+W_s)_{,xx}+2\cos\theta\sin\theta(W_b+W_s)_{,yx}+\sin^2\theta(W_b+W_s)_{,yy}\right)\\
&-G_\eta\left(\sin^2\theta(W_b+W_s)_{,xx}-2\sin\theta\cos\theta(W_b+W_s)_{,yx}+\cos^2\theta(W_b+W_s)_{,yy}\right)
\end{aligned}
$$

$$
\begin{aligned}
&+P\cos(\omega T)(\frac{\partial^2}{\partial Y^2}W_b+\frac{\partial^2}{\partial Y^2}W_s)^2-I_0(\frac{\partial^2}{\partial T^2}W_b+\frac{\partial^2}{\partial T^2}W_s)\\
&\left.+F\cos(\Omega T)(\frac{\partial^2}{\partial X^2}W_b+\frac{\partial^2}{\partial X^2}W_s)-J_1(\frac{\partial}{\partial X}\frac{\partial^2}{\partial T^2}U+\frac{\partial}{\partial X}\frac{\partial^2}{\partial T^2}V\right]=0
\end{aligned}
\tag{24}
$$

3. DQM

In this method, the differential equations are changed into a first order algebraic equation by employing appropriate weighting coefficients. Because weighting coefficients do not relate to any special problem and only depend on the grid spacing. In other words, the partial derivatives of a function (say w here) are approximated with respect to specific variables (say x and y), at a discontinuous point in a defined domain ($0<x<L_x$ and $0<y<L_y$) as a set of linear weighting coefficients and the amount represented by the function itself at that point and other points throughout the domain. The approximation of the n^{th} and m^{th} derivatives function with respect to x and y , respectively may be expressed in general form as (Ghorbanpour Arani, Kolahchi *et al.* 2012)

$$
\begin{aligned}
&f_x^{(n)}(x_i,y_i)=\sum_{k=1}^{N_x}A^{(n)}{}_{ik}\,f(x_k,y_j),\\
&f_y^{(m)}(x_i,y_i)=\sum_{l=1}^{N_y}B^{(m)}{}_{jl}\,f(x_i,y_l),\\
&f_{xy}^{(n+m)}(x_i,y_i)=\sum_{k=1}^{N_x}\ \sum_{l=1}^{N_y}A^{(n)}{}_{ik}B^{(m)}{}_{jl}\,f(x_k,y_l),
\end{aligned}
\tag{25}
$$

where N_x and N_y, denotes the number of points in x and $y$directions, $f(x,y)$ is the function and A_{ik}, B_{jl} are the weighting coefficients defined as

$$
\begin{aligned}
A^{(1)}{}_{ij}&=\frac{M(x_i)}{(x_i-x_j)M(x_j)},\\
B^{(1)}{}_{ij}&=\frac{P(y_i)}{(y_i-y_j)M(y_j)},
\end{aligned}
\tag{26}
$$

where M and P are Lagrangian operators defined as

$$
\begin{aligned}
M(x_i)&=\prod_{j=1}^{N_x}(x_i-x_j),\quad i\neq j\\
P(y_i)&=\prod_{j=1}^{N_y}(y_i-y_j),\quad i\neq j.
\end{aligned}
\tag{27}
$$

The weighting coefficients for the second, third and fourth derivatives are determined via matrix multiplication

$$A^{(2)}{}_{ij}=\sum_{k=1}^{N_x}A^{(1)}{}_{ik}A^{(1)}{}_{kj},\ A^{(3)}{}_{ij}=\sum_{k=1}^{N_x}A^{(2)}{}_{ik}A^{(1)}{}_{kj},\ A^{(4)}{}_{ij}=\sum_{k=1}^{N_x}A^{(3)}{}_{ik}A^{(1)}{}_{kj},\quad i,j=1,2,...,N_x,$$
$$B^{(2)}{}_{ij}=\sum_{k=1}^{N_y}B^{(1)}{}_{ik}B^{(1)}{}_{kj},\ B^{(3)}{}_{ij}=\sum_{k=1}^{N_y}B^{(2)}{}_{ik}B^{(1)}{}_{kj},\ B^{(4)}{}_{ij}=\sum_{k=1}^{N_y}B^{(3)}{}_{ik}B^{(1)}{}_{kj},\quad i,j=1,2,...,N_y. \tag{28}$$

Using the following rule, the distribution of grid points in domain is calculated as

$$x_i=\frac{L_x}{2}[1-\cos(\frac{\pi i}{N_x})],$$
$$y_j=\frac{L_y}{2}[1-\cos(\frac{\pi j}{N_y})], \tag{29}$$

Let the in-plane load P be periodic and may be expressed as

$$P(t)=\alpha P_{cr}+\beta P_{cr}\cos(\omega t), \tag{30}$$

where ω is the frequency of excitation, P_{cr} is the static buckling load, α and β may be defined as static and dynamic load factors, respectively. Now Eq. (26) can be written as

$$\{[K-\alpha P_{cr}K_G-\beta P_{cr}\cos(\omega t)K_G][d]+[C][\dot{d}]+[M][\ddot{d}]\}=[0], \tag{31}$$

In order to determinate the boundaries of dynamic instability regions, the method suggested by Bolotin (1964) is applied. Hence, the components of $\{d\}$ can be written in the Fourier series with period $2T$ as

$$\{d\}=\sum_{k=1,3,...}^{\infty}\left[\{a\}_k\sin\frac{k\omega t}{2}+\{b\}_k\cos\frac{k\omega t}{2}\right], \tag{32}$$

According to this method, the first instability region is usually the most important in studies of structures. It is due to the fact that the first DIR is wider that other DIRs and structural damping in higher regions becomes neutralize (Lanhe, Hongjun *et al*. 2007). Substituting Eq. (32) into Eq. (31) and setting the coefficients of each sine and cosine as well as the sum of the constant terms to zero, yields

$$\left|\left([K_L+K_{NL}]-P_{cr}\alpha[K]_G\pm P_{cr}\frac{\beta}{2}[K]_G\mp[C]\frac{\omega}{2}-[M]\frac{\omega^2}{4}\right)\right|=0\ . \tag{33}$$

Solving the above equation based on eigenvalue problem, the variation of ω with respect to α can be plotted as DIR.

4. Results and discussion

In this section, the nano-plate is composed of aluminum (as metal) and alumina (as ceramic). The Young's modulus and density of aluminum are E_m=70 Gpa and ρ_m=2702 kg/m^3 respectively, and those of alumina are E_c=380 Gpa and ρ_c=3800 kg/m^3 respectively.

Table 1 Comparison of this work with Hosseini-Hashemi *et al*. (2011a, 2011b)

a/h	Method	Power law index (*p*)						
		0	0.5	1	2	5	8	10
5	FSDT, (2011a)	3.4409	2.9322	2.6473	2.4017	2.2528	2.1985	2.1677
	TSDT, (2011b)	3.4412	2.9347	2.6475	2.3949	2.2272	2.1697	2.1407
	present	3.4416	2.9350	2.6478	2.3948	2.2260	2.1688	2.1403
10	FSDT, (2011a)	3.6518	3.0983	2.7937	2.5386	2.3998	2.3504	2.3197
	TSDT, (2011b)	3.6518	3.0990	2.7937	2.5364	2.3916	2.3411	2.3110
	present	3.6519	3.0991	2.7937	2.5364	2.3912	2.3408	2.3108
20	FSDT, (2011a)	3.7123	3.1456	2.8352	2.5777	2.4425	2.3948	2.3642
	TSDT, (2011b)	3.7123	3.1458	2.8352	2.5771	2.4403	2.3923	2.3619
	present	3.7123	3.1458	2.8353	2.5771	2.4401	2.3922	2.3618

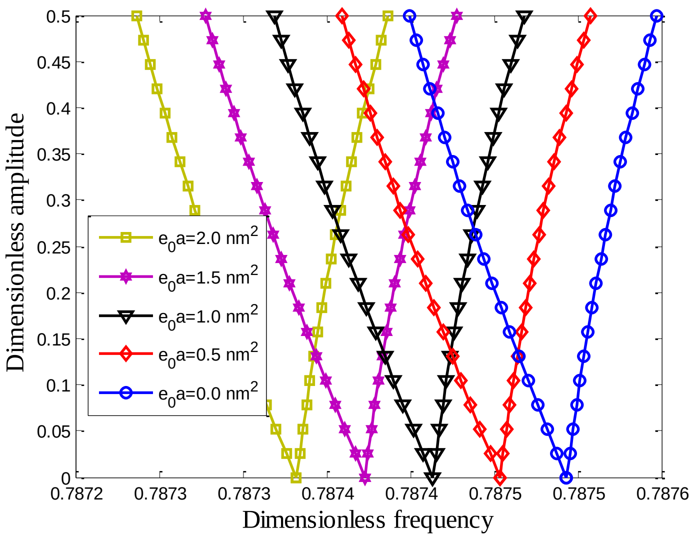

Fig. 2 Dimensionless pulsation amplitude versus dimensionless pulsation frequency for different nonlocal parameters

To the best of the authors' knowledge no published literature is available for viscoelastic FGM nano-plate embedded in an orthotropic visco-Pasternak foundation based on SSDT. Since, no reference to such a work is found to-date in the literature, its validation is not possible. However, in an attempt to validate this work as far as possible, a simplified analysis of this paper is carried out without considering the nonlocal parameter, orthotropic visco-Pasternak foundation and viscoelastic property of system. Present results are compared with the work of Hosseini-Hashemi, Fadaee *et al*. (2011a, 2011b) based on Third-order shear deformation theory (TSDT) and First-order shear deformation theory (FSDT), respectively. Considering the material properties the same as Hosseini-Hashemi, Fadaee *et al*. (2011a, 2011b) and dimensionless frequency as $\bar{\omega} = \omega h\sqrt{\rho_C / E_C}$, the results of comparison are shown in Table 1.As can be seen, present results are in good agreement with Hosseini-Hashemi, Fadaee *et al*. (2011a, 2011b), indication validation of this work.

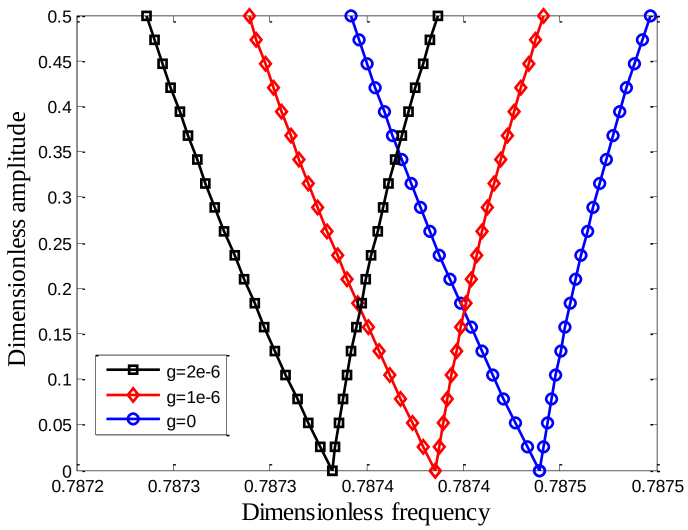

Fig. 3 Dimensionless pulsation amplitude versus dimensionless pulsation frequency for different structural damping constants

Generally, in all of the following figures, in order to show the DIR, the pulsation frequency is plotted against pulsation amplitude. In these figures, the regions inside and outside the boundary curves correspond to unstable (parametric resonance) and stable regions, respectively.

Fig. 2 demonstrates the graph of DIR for different the nonlocal parameters. It can be found that the frequency of the system decreases as the nonlocal parameter is increased. It means that with increasing nonlocal parameter, DIR of system happens in lower frequencies. This is because increasing the nonlocal parameter implies decreasing interaction force between nano-plate atoms leads to a softer structure. In addition, with increasing nonlocal parameter, the instability region of system becomes smaller.

Fig. 3 demonstrates the DIR for different structural damping constant. As can be seen, the DIR and natural frequency of visco-nanoplate are lower than those of non-visco-nanoplate (i.e., g=0). This remarkable difference show that considering the nature of FGM nanoplate as viscoelastic can yield the accurate results with respect to non-visco-nanoplate. The reason is that assuming viscoelastic nano-plate means induce of damping force which results in more absorption of vibration energy by the nano-plate.

The influences of the viscoelastic medium type on the DIR of system are shown in Fig. 4. As can be seen considering elastic medium increases the frequency of FGM visco-nanoplate. This is due to the fact that considering elastic medium leads to a stiffer structure. The frequency predicted by visco-Pasternak-type is higher than the visco-Winkler-type. It is perhaps due to the fact that the Winkler-type is capable to describe just normal load of the elastic medium while the Pasternak-type describes both transverse shear and normal loads of the elastic medium.

The effect of power index of FG model on the DIR of the nano structure is shown in Fig. 5. It is obvious that with increasing power index of FG model, the instability region happens in higher pulsation frequencies.

In realizing the influence of boundary conditions, Fig. 6 shows how the pulsation frequency changes with respect to pulsation amplitude. It is found that the frequency of the system for CCCC

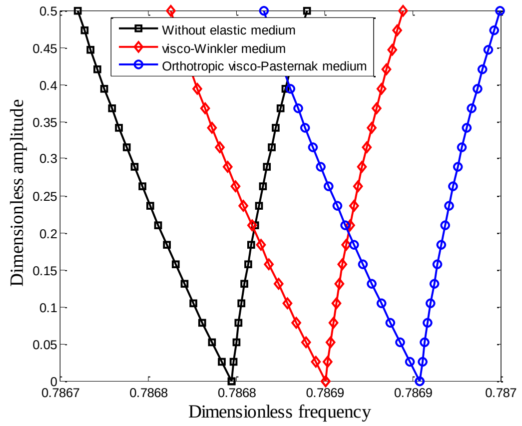

Fig. 4 Dimensionless pulsation amplitude versus dimensionless pulsation frequency for different elastic medium

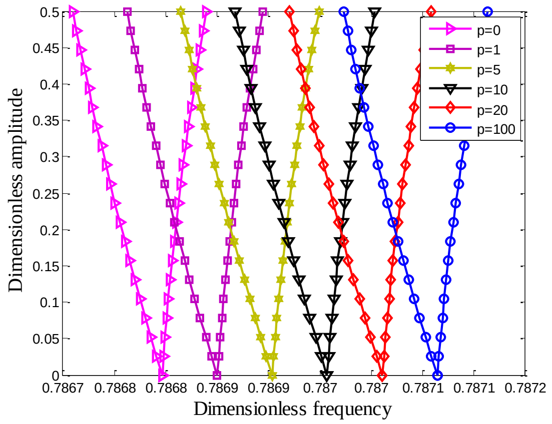

Fig. 5 Dimensionless pulsation amplitude versus dimensionless pulsation frequency for different power index of FG model

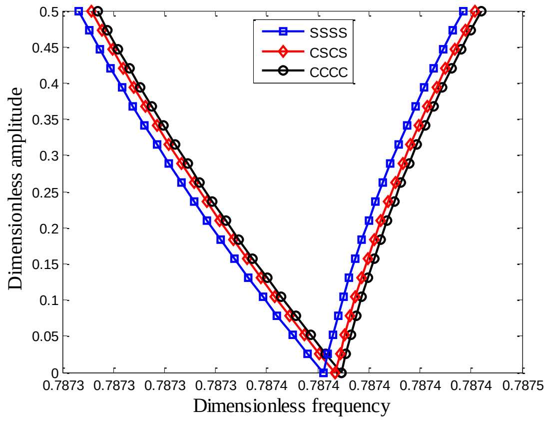

Fig. 6 Dimensionless pulsation amplitude versus dimensionless pulsation frequency for different boundary conditions

and SSSS boundary conditions is maximum and minimum, respectively. It is due to the fact that the stability of system if maximum in CCCC boundary condition case.

5. Conclusions

Dynamic response of nano-plates has applications in designing many NEMS/MEMS devices. Biaxial harmonic load induced dynamic instability of FGM nano-plates considering structural damping and orthotropic viscoelastic foundation was the main contributions of the present paper. The FGM nano-platesare simulated by SSDT and size effects were considered using Eringen's nonlocal theory. Bolotin method in conjunction with DQM were used for calculating the DIR of the viscoelastic FGM nano-plates so that the effects of nonlocal parameter, orthotropic visco-Pasternak foundation, power index of FG model, structural damping and boundary conditions were discussed. Results depict that considering the nature of FGM nano-plate as viscoelastic can yield the accurate results with respect to non-visco-nanoplate. Furthermore, the frequency of the system decreases as the nonlocal parameter was increased. In addition, with increasing power index of FG model, the instability region happens in higher pulsation frequencies. The results of this study were in good agreement with those reported by Hosseini-Hashemi, Fadaee *et al*. (2011a, 2011b). The results presented in this work can be useful for the study and design of the next generation of nano/micro structures that make use of the nonlocal dynamic instability of viscoelastic FGM nano-plate embedded in viscoelastic medium.

Acknowledgments

The author would like to thank the reviewers for their comments and suggestions to improve the clarity of this article. The authors are grateful to University of Kashan for supporting this work by Grant No. 574600/11. They would also like to thank the Iranian Nanotechnology Development Committee for their financial support.

References

Amabili, M. (2004), "Nonlinear vibrations of rectangular plates with different boundary conditions: theory and experiments", *Comput. Struct.*, **82**, 2587-2605.

Bolotin, V.V. (1964), "The dynamic stability of elastic systems. in: the dynamic stability of elastic systems", Holden-Day, San Francisco.

Chakraverty, S. and Behera L. (2015), "Small scale effect on the vibration of non-uniform nanoplates", *Struct. Eng. Mech.*, **55**, 495-510.

Chien, R.D. and Chen, C.S. (2006), "Nonlinear vibration of laminated plates on an elastic foundation", *Thin Wall. Struct.*, **44**, 852-860.

Ebraheem, O., Ashraf, A. and Zenkour, M. (2013), "Small scale effect on hygro-thermo-mechanical bending of nanoplates embedded in an elastic medium", *Compos. Struct.*, **105**, 163-172.

Ebrahimi, F. and Salari, E. (2015), "Nonlocal thermo-mechanical vibration analysis of functionally graded nanobeams in thermal environment", *Acta Astronaut.*, **113**, 29-50.

Eringen, A.C. (1983), "On differential equations of nonlocal elasticity and solutions of screw dislocation and surface waves", *J. Appl. Phys.*, **54**, 4703-4710.

Ghorbanpour Arani, A., Kolahchi, R., Mosallaie Barzoki, A.A., Mozdianfard, M.R. and Noudeh Farahani, S.M. (2012), “Elastic foundation effect on nonlinear thermo-vibration of embedded double-layered orthotropic grapheme sheets using differential quadrature method”, *Inst. Mech. Eng. Part C, J. Mech. Eng. Sci*., **227**, 862-879.

Ghorbanpour Arani, A., Mosallaie Barzoki, A.A., Kolahchi, R. and Loghman, A. (2011), “Pasternak foundation effect on the axial and torsional waves propagation in embedded DWCNTs using nonlocal elasticity cylindrical shell theory”, *J. Mech. Sci. Tech*., **25**, 2385-2391.

Hosseini-Hashemi, S., Fadaee, M. and Atashipour, S.R. (2011a), “A new exact analytical approach for free vibration of Reissner-Mindlin functionally graded rectangular plates”, *Int. J. Mech. Sci*., **53**, 11-22.

Hosseini-Hashemi, S., Fadaee, M. and Atashipour, S.R. (2011b), “Study on the free vibration of thick functionally graded rectangular plates according to a new exact closed-form procedure”, *Compos. Struct*., **93**, 722-735.

Karličić, D., Adhikari, S., Murmu, T. and Cajić, M. (2014), “Exact closed-form solution for non-local vibration and biaxial buckling of bonded multi-nanoplate system”, *Compos. Part B: Eng*., **66**, 328-339.

Kutlu, A. and Omurtag, M.H. (2012), “Large deflection bending analysis of elliptic plates on orthotropic elastic foundation with mixed finite element method”, *Int. J. Mech. Sci*., **65**, 64-74

Lanhe, W., Hongjun, W. and Daobin, W. (2007), “Dynamic stability analysis of FGM plates by the moving least squares differential quadrature method”, *Compos. Struct*., **77**, 383-394.

Lei, J., He, Y., Zhang, B., Gan, Z. and Zeng, P.C. (2013a), “Bending and vibration of functionally graded sinusoidal microbeams based on the strain gradient elasticity theory”, *Int. J. Eng. Sci*., **72**, 36-52.

Lei, Y., Adhikari, S. and Friswell, M.I. (2013b), “Vibration of nonlocal Kelvin-Voigt viscoelastic damped Timoshenko beams”, *Int. J. Eng. Sci*., **66**, 1-13.

Li, J.J. and Cheng, C.J. (2005), “Differential quadrature method for nonlinear vibration of orthotropic plates with finite deformation and transverse shear effect”, *J. Sound Vib*., **281**, 295-309.

Lu, P., Zhang, P.Q., Lee, H.P., Wang, C.M. and Reddy, J.N. (2007), “Non-local elastic plate theories”, *Proc. R. Soc. A*, **463**, 3225-3240.

Malekzadeh, P. (2008), “Nonlinear free vibration of tapered Mindlin plates with edges elastically restrained against rotation using DQM”, *Thin Wall. Struct*., **46**.11-26.

Nami, M.R. and Janghorban, M. (2013), “Static analysis of rectangular nanoplates using trigonometric shear deformation theory based on nonlocal elasticity theory”, *Beilstein J. Nanotechnol*., **4**, 968-973.

Nami, M.R. and Janghorban, M. (2014), “Static analysis of rectangular nanoplates using exponential shear deformation theory based on strain gradient elasticity theory”, *Iran. J. Mat. Form*., **1**, 1-13.

Narendar, S. (2011), “Buckling analysis of micro/nano-scale plates based on two-variable refined plate theory incorporating nonlocal scale effects”, *Compos. Struct*., **93**, 3093-3103.

Wang, Y.Z. and Li, F.M. (2012), “Static bending behaviors of Nanoplate embedded in elastic matrix with small scale effects”, *Mech. Res.Commun*., **41**, 44-48.

Zenkour, A.M. (2009), “The refined sinusoidal theory for FGM plates on elastic foundations”, *Int. J. Mech. Sci*., **51**, 869-880.

CC